GA–A24867

100% NONINDUCTIVE OPERATION AT HIGH BETA USING OFF-AXIS ECCD

by
M. MURAKAMI, C.M. GREENFIELD, M.R. WADE, T.C. LUCE, J.R. FERRON, H.E. ST JOHN, M.A. MAKOWSKI, M.E. AUSTIN, S.L. ALLEN, D.P. BRENNAN, K.H. BURRELL, T.A. CASPER, J.C. DeBOO, E.J. DOYLE, A.M. GAROFALO, P. GOHIL, I.A. GORELOV, R.J. GOEBNER, J. HOBIRK, A.W. HYATT, R.J. JAYAKUMAR, K. KAJIWARA, C.E. KESSEL, J.E. KINSEY, R.J. LA HAYE, J.Y. KIM, L.L. LAO, J. LOHR, J.E. MENARD, C.C. PETTY, T.W. PETRIE, R.I. PINSKER, P.A. POLITZER, R. PRATER, T.L. RHODES, A.C.C. SIPS, G.M. STAEBLER, T.S. TAYLOR, G. WANG, W.P. WEST, L. ZENG, and the DIII–D TEAM

OCTOBER 2004

DISCLAIMER

GA–A24867

100% NONINDUCTIVE OPERATION AT HIGH BETA USING OFF-AXIS ECCD

by
M. MURAKAMI,* C.M. GREENFIELD, M.R. WADE,* T.C. LUCE, J.R. FERRON, H.E. ST JOHN, M.A. MAKOWSKI,† M.E. AUSTIN,‡ S.L. ALLEN,† D.P. BRENNAN,Δ K.H. BURRELL, T.A. CASPER,† J.C. DeBOO, E.J. DOYLE,# A.M. GAROFALO,¶ P. GOHIL, I.A. GORELOV, R.J. GOEBNER, J. HOBIRK,§ A.W. HYATT, R.J. JAYAKUMAR,† K. KAJIWARA,Δ C.E. KESSEL,∞ J.E. KINSEY,□ R.J. LA HAYE, J.Y. KIM, L.L. LAO, J. LOHR, J.E. MENARD,∞ C.C. PETTY, T.W. PETRIE, R.I. PINSKER, P.A. POLITZER, R. PRATER, T.L. RHODES,# A.C.C. SIPS,§ G.M. STAEBLER, T.S. TAYLOR, G. WANG,# W.P. WEST, L. ZENG,# and the DIII–D TEAM

This is a preprint of a paper to be presented at the 20th IAEA Fusion Energy Conference, Vilamoura, Portugal, November 1–6, 2004 and to be published in the *Proceedings.*

*Oak Ridge National Laboratory, Oak Ridge, Tennessee.
†Lawrence Livermore National Laboratory, Livermore, California.
‡University of Texas, Austin, Texas.
ΔOak Ridge Institute for Science Education, Oak Ridge, Tennessee.
#University of California – Los Angeles, Los Angeles, California.
¶Columbia University, New York, New York.
§Max-Planck-Institut for Plasmaphysiks, Garching, Germany.
∞Princeton Plasma Physics Laboratory, Princeton, New Jersey.
□Lehigh University, Bethlehem, Pennsylvania.

Work supported by
the U.S. Department of Energy
under DE-AC05-00OR22725, DE-FC02-04ER54698, W-7405-ENG-48, DE-FG03-97ER54415, DE-AC05-76OR00033, DE-FG03-01ER54615, DE-FG02-89ER53297, DE-AC02-76CH03073, and DE-FG02-92ER54141

GENERAL ATOMICS PROJECT 30200
OCTOBER 2004

100% Noninductive Operation at High Beta Using Off-axis ECCD

M. Murakami,[1] C.M. Greenfield,[2] M.R. Wade,[1] T.C. Luce,[2] J.R. Ferron,[2] H.E. St John,[2] M.A. Makowski,[3] M.E. Austin,[4] S.L. Allen,[3] D.P. Brennan,[5] K.H. Burrell,[2] T.A. Casper,[1] J.C. DeBoo,[2] E.J. Doyle,[6] A.M. Garofalo,[7] P. Gohil,[2] I.A. Gorelov,[2] R.J. Groebner,[2] J. Hobirk,[8] A.W. Hyatt,[2] R.J. Jayakumar,[3] K. Kajiwara,[9] C.E. Kessel,[10] J.E. Kinsey,[11] R.J. La Haye,[2] J.Y. Kim,[2] L.L. Lao,[2] J. Lohr,[2] J.E. Menard,[10] C.C. Petty,[2] T.W. Petrie,[2] R.I. Pinsker,[2] P.A. Politzer,[2] R. Prater,[2] T.L. Rhodes,[6] A.C.C. Sips,[8] G.M. Staebler,[2] T.S. Taylor,[2] G. Wang,[6] W.P. West,[2] L. Zeng,[6] and the DIII–D Team

[1]Oak Ridge National Laboratory, Oak Ridge, Tennessee,USA
[2]General Atomics, P.O. Box 85608, San Diego, California, USA
[3]Lawrence Livermore National Laboratory, Livermore, California, USA
[4]University of Texas at Austin, Austin, Texas, USA
[5]Massachusetts Institute of Technology, Cambridge, Massachusetts, USA
[6]University of California at Los Angeles, Los Angeles, California, USA
[7]Columbia University, New York, New York, USA
[8]Max-Planck-Institut for Plasmaphysiks, Garching, Germany
[9]Oak Ridge Institute for Science Education, Oak Ridge, Tennessee, USA
[10]Princeton Plasma Physics Laboratory, Princeton, New Jersey, USA
[11]Lehigh University, Bethlehem, Pennsylvania, USA

e-mail contact of main author: murakami@fusion.gat.com

Abstract. The Advanced Tokamak (AT) program on DIII-D is developing the scientific basis for steady-state, high-performance operation in future devices. The key element of the program is to demonstrate sustainment of 100% noninductive current for several seconds at high beta. Guided by integrated modeling, recent experiments using up to 2.5 MW of off-axis electron cyclotron current drive (ECCD) and up to 15 MW neutral beam injection (NBI) with $q_{95} \approx 5$ have sustained ≈100% of the plasma current noninductively for 1 s at high beta ($\beta \approx 3.6\%$, $\beta_N \approx 3.4$, above the no-wall limit) with $q_{min} \geq 1.5$ and good confinement ($H_{89} \approx 2.3$). Integrated modeling using both empirical and theory-based models is used to design experiments and to interpret their results. These experiments have achieved the parameters required for the ITER Q=5 steady-state scenario, and the same modeling tools are applied to ITER AT scenario development.

1. Introduction

Advanced Tokamak (AT) research in DIII-D seeks to provide a scientific basis for steady-state, high performance operation in future devices [1]. For steady-state operation, all of the plasma current must be supplied by noninductive means. A high fraction of the self-generated bootstrap current [2], $f_{BS} = I_{BS}/I_p \propto \beta_p = q\beta_N$, is desirable to minimize the re-circulating power, but it must also be well aligned with the desired current profile. Here $\beta_N = \beta_T a B_T/I_p$ where β_T is in %, I_p (MA) is the plasma current, a (m) is the plasma minor radius and B_T (T) is the toroidal field. The need for a well aligned bootstrap current further constrains the plasma conditions: not only should β_p be large, but the kinetic profiles must also be broad to optimize the alignment. The remainder of the plasma current is provided by external, noninductive means. High fusion gain ($\beta_T\tau_E$) requires high values of normalized β_N and high confinement, H_{89}, at a modest safety factor, q,where H_{89} is the ratio of energy confinement time (τ_E) relative to ITER L-mode scaling [3]. These requirements can be combined into an ignition figure of merit, $G = \beta_N H/q^2$ [4].

Toward these goals, AT experiments on DIII-D uniquely strive to integrate the key elements that are required for sustained AT operation: high β operation at modest q, high confinement, and efficient current drive. These experiments take advantage of recent improvements on DIII-D. Resistive wall mode (RWM) stabilization via plasma rotation and active feedback with non-axisymmetric coils allows routine operation above the no-wall beta limit [5]. Neoclassical tearing modes (NTMs) are avoided through current profile control, although

active feedback stabilization using localized electron cyclotron current drive (ECCD) [6] has also been demonstrated. ECCD is an integral part of the experiment to drive current at the mid-radius to sustain the favorable configuration. Density control of AT discharges with an edge localized modes (ELMs) using divertor cryopumps facilitates high current drive efficiency at reactor relevant collisionality. An advanced plasma control system allows integrated control of these elements.

Modeling and simulation guide the DIII-D AT program. Understanding the detailed current profile evolution is crucial to extending high performance plasmas to steady state. The main limitation to the duration of high performance discharges is the current profile evolution. Understanding the evolution is an interesting scientific challenge because of the complex interactions amongst the bootstrap current, external current drive, transport and magnetohydrodynamic (MHD) stability. This requires integrated modeling tools, and these tools need to be validated against experiments. Using both empirical and physics-based models, AT experiments are both planned and interpreted in light of these simulations. The modeling effort benefits both the experiments and the models, since the results guide the development of both. This supports one of our major goals: to develop a predictive capability that can be applied to the design of advanced scenarios in next-step burning plasma experiments.

In this paper, we discuss the status of experimental efforts toward an integrated demonstration of 100% noninductive operation at high beta, and key elements required for its success. We discuss then an exploitation of a unique capability of a modeling tool for predicting steady state performance in DIII-D and ITER.

2. The Experiment

Significant progress has been made since the last Fusion Energy Conference in achieving and extending ~100% noninductive plasmas. Figure 1(a) (open symbols) shows a global parameter database assembled in the ITPA database format [7] which includes about 80 DIII-D AT discharges. Since 2002, the operating space for the AT regime has expanded significantly toward higher β_p at the ignition figure of merit $G \equiv \beta_N H/q_{95}^2$ relevant to the ITER reference Q~5 noninductive scenario [8] and that of our simulation work for ITER which will be discussed later. A great deal of detailed analysis beyond the global parameters is required for understanding the discharge profile evolution. Detailed profile analysis and simulations have been carried out for a smaller number of shots indicated by solid symbols. Figure 1(b) shows the noninductive current fraction as a function of the noninductive duration τ_{dur}^{NI} normalized to the current

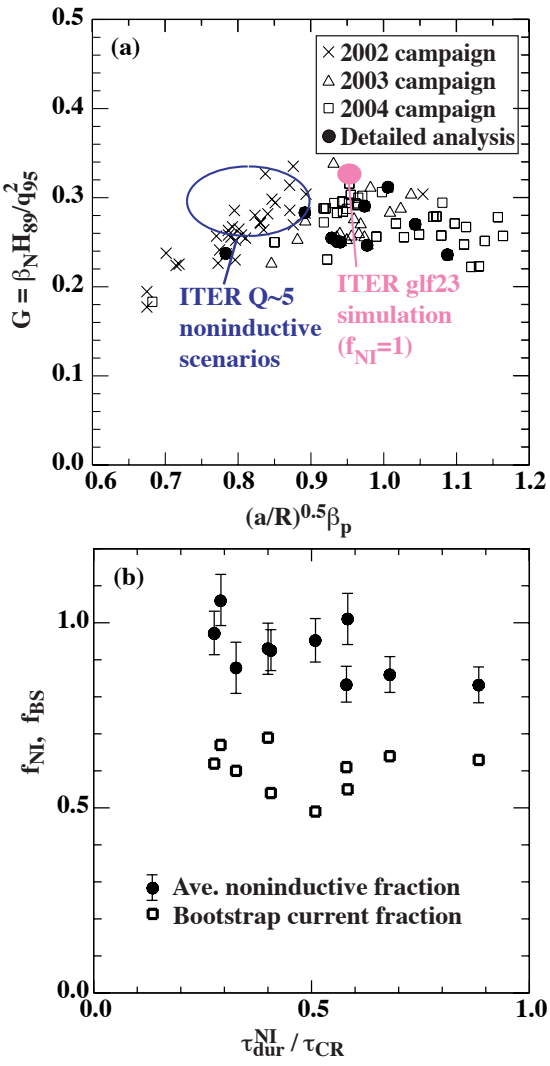

Fig. 1. (a) Operating space of the ignition figure of merit ($\beta_N H_{89}/q^2$) vs. bootstrap current fraction index ($a/R^{1/2}\beta_p$) in the ITPA database format has expanded substantially in the recent DIII-D AT operation. Also shown are the target operating space for the ITER $Q \sim 5$ noninductive operation and that of our GLF23 model prediction. (b) Detailed analysis has identified several shots with 100% noninductive fraction, and >60% bootstrap current fraction.

redistribution time τ_{CR} [9]. Here, the noninductive duration τ_{dur}^{NI} is defined as the period with f_{NI} above 85% of the highest noninductive fraction indicated by transport analysis of each discharge, and the noninductive fraction is a fraction averaged over that period, with RMS values as error bars. A number of discharges have achieved 100% noninductive fraction with ~60% bootstrap current fraction. We will discuss more detailed analysis of a few representative discharges and their limitations.

Full noninductive at increased beta was obtained by careful modeling and extension of previous experiment reported at the last Fusion Energy Conference [10] with $q_{min} > 1.5$, $\beta_N = 3.1$, $f_{BS} \sim 60\%$. Predictive modeling [11] using both scaled-experimental [12] and theory-based GLF23 [13] transport models indicated that increasing the neutral beam power would result in plasmas reaching a noninductive current fraction $f_{NI} \approx 100\%$ at higher β. Experiments have been carried out to test these predictions. Using 2.5 MW of off-axis (ρ = 0.4-0.5) ECCD and up to 15 MW NBI with $q_{95} = 5.0$, nearly 100% of the plasma current has been sustained for 0.5 s at high beta ($\beta \approx 3.6\%$, $\beta_N \approx 3.4$, slightly above the empirical no-wall limit, $4l_i$ where l_i is the internal inductance) with $q_{min} > 1.5$, as shown in Fig. 2. The loop voltage was reduced to near zero during this phase.

The details of the current profile in these discharges were analyzed using different codes and different bootstrap models. ONETWO [14] and TRANSP [15] are both transport codes. In these calculations, the bootstrap current is determined using the NCLASS [16] or Sauter [17] model. Neutral beam driven current is calculated using models internal to the codes. ECCD is calculated using TORAY-GA [18]. The Ohmic current density is then determined by subtracting these calculated noninductive currents from the total current which is calculated from a reconstruction of the plasma equilibrium using EFIT [19].

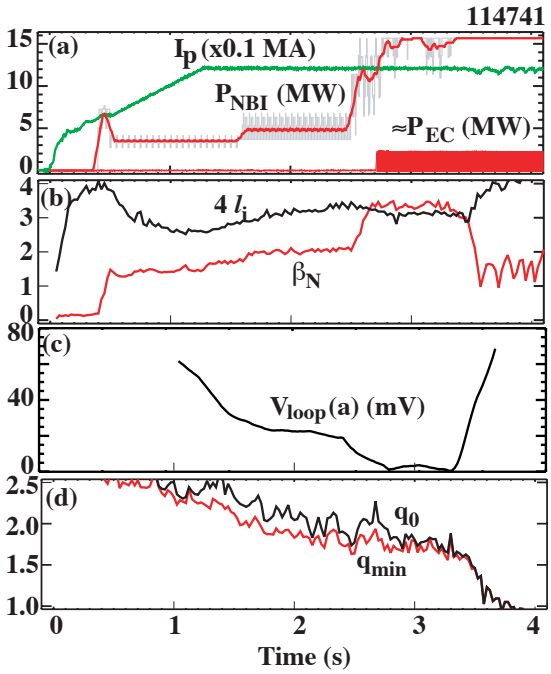

Fig. 2. Time histories of discharge parameters of a typical *AT* discharge with $f_{NI} \approx 100\%$, $\beta_N \approx 3.5$ and $\beta_T \approx 3.6$ %. High performance ends due to an n=1 tearing mode which begins at 3.236 s.

An alternate method of calculating the current density profile uses the NVLOOP code [20]. The poloidal flux, $\Psi(\rho,t)$ is given by a series of equilibrium reconstructions with a fine time resolution based on the MSE diagnostic and magnetic measurements incorporated with pressure profiles. The total current is given by spatial derivatives of Ψ, while the Ohmic current J_{OH} is given by $\sigma_{neo} E_{||}$, where σ_{neo} is the neoclassical conductivity and $E_{||}$ is the parallel electric field determined by the time derivative of Ψ. The noninductive current can be calculated by subtracting the Ohmic current from the total current, and can be compared with the sum of ECCD, neutral beam current drive (NBCD) and bootstrap currents as described above.

Figure 3(a) shows results of such calculations from TRANSP and ONETWO (using the Sauter bootstrap formulation) and NVLOOP for the discharge shown in Fig. 2. The noninductive current fraction f_{NI} indicates that this discharge is nearly 100% noninductively sustained for ~0.7 s which corresponds to 0.3 τ_{CR}. A snapshot of the components of the current profile near the end of the ECCD pulse is shown in Fig. 3(b), indicating that although the total current (integrated over the cross section of the plasma) is nearly 100% noninductive, locally, this is not the case.

The details of the different components of the current density depend on the complex interaction amongst the transport (confinement), and the stability limits. A lower confinementtime requires more neutral beam power to reach the target beta and thus the excess axial beam current. To reach and maintain f_{NI} ~1, both globally and locally, a certain amount of NBCD is needed, which often will be different than the amount determined by confinement. These discharges had a higher power demand (lower confinement, $H_{89} \approx$ 1.9 instead of $H_{89} \approx$ 2.3-2.4) than the previous discharges, and so $J_{tot}(\rho)$ in the region surrounding the magnetic axis is overdriven by NBCD [Fig. 3(b)]. The Ohmic current density, counter to the total current, is a direct response to this NBCD overdrive.

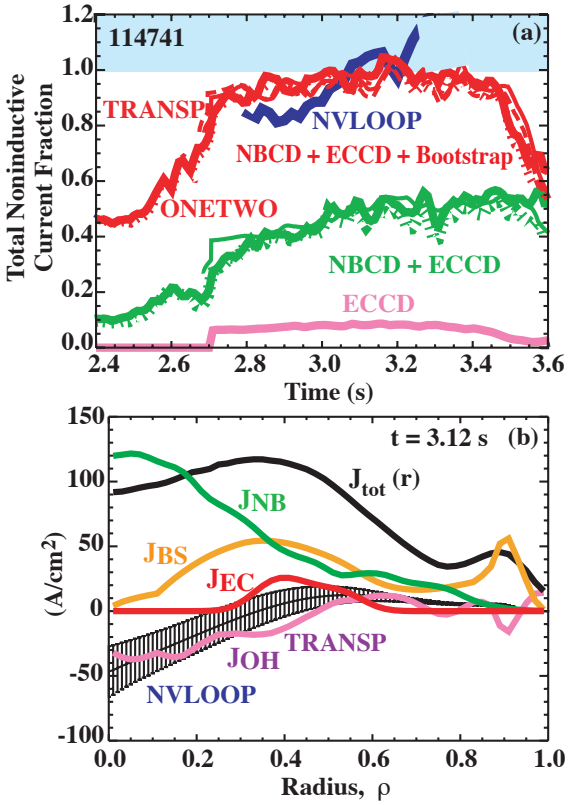

Fig. 3. (a) The net noninductive current fraction ~100% is maintained for over 0.5 s with off-axis ECCD in the discharge shown in Fig. 2. (b) The radial profile of the components of the current are shown. Near the axis of these plasmas, neutral beam current drive actually overdrives the total current, resulting in Ohmic counter-current to balance the noninductive sources.

Lower than optimum confinement might be associated with reduced toroidal rotation as a consequence of momentum drag from a residual nonaxisymmetric field, and a non-optimal q profile. Self-consistent simulations using the transport model GLF23 [21] in the code ONETWO indicate that the important difference is the toroidal rotation. The T_e, T_i, and toroidal momentum equations are solved with self-consistent source and sink calculations by time stepping from initial profiles over several confinement times. The density profile is fixed using the experimentally measured profile at a given time. Figure 4 shows the resulting profiles that are in good agreement with experimental profiles in the high confinement discharge (111221). A simulation, using GLF23, of a low confinement shot (115689) [22] with higher NB power request (P_{NBI} = 14 MW as opposed to 9.4 MW, corresponding to H_{89} = 1.9 and 2.3, respectively), shows that the predictived toroidal rotation is higher by about 50% than the experiment, as shown in Fig. 5. The T_e and T_i are also overestimated by about 20%. Recent GLF23 simulations using XPTOR solving the additional electron density equation arrived at a similar difference between "high" and "low" confinement discharges [22]. A possible explanation for the discrepancy between the simulation and experiment is drag due to the magnetic error fields and/or RWM effects missing in the toroidal momentum equation. The simulation also predicts improved confinement due to the more negative central shear configuration rather than nearly monotonic q-profiles that occurred in the low confinement shots. However, the effect of the q profile is rather modest, and we believe the important difference is that seen in the toroidal rotation. This motivated efforts to improve RWM feedback (and magnetic shear) in the subsequent experiments.

Good confinement was recovered with improved error field compensation and RWM feedback in the 2004 experiments, allowing the exploration of higher β_p region of operating space with limited ECCD power (2.1 MW). Figure 6 shows time histories of a typical discharge. The flat top I_p was reduced to 1.1 MA (from 1.2 MA) at B_T = 1.85 T. The β_N NBI feedback was initiated early in the discharge to improve shot-to-shot reproducibility. The high β phase was delayed until q_{min} dropped below 2, followed by the addition of ECCD aimed at ρ = 0.4. The edge loop voltage remained low (~10 mV) until a large-

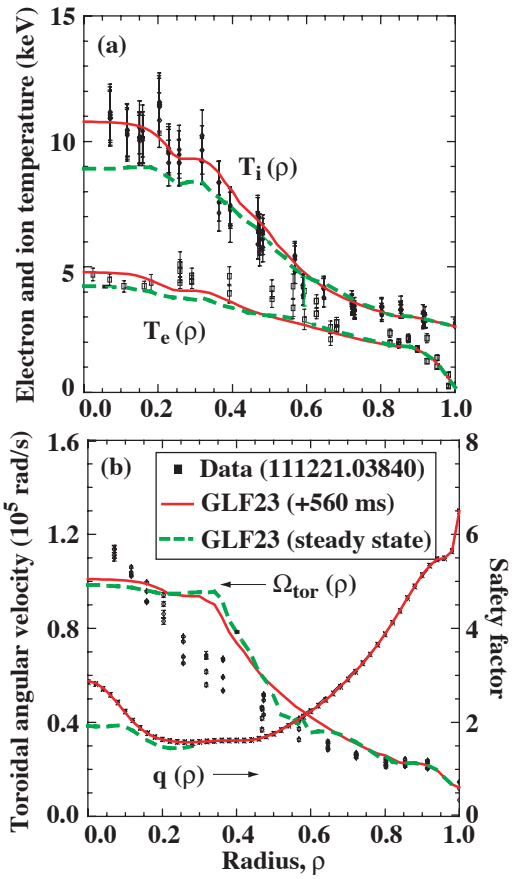

Fig. 4. GLF23 model predictions are compared with experimental profiles for the ≈90% noninductive AT discharge in DIII-D. Solid curves are predicted profiles with time-dependent simulation for 0.56 s after starting with the initial experimental profiles, and dashed curves are steady-state predictions including the poloidal magnetic field equation.

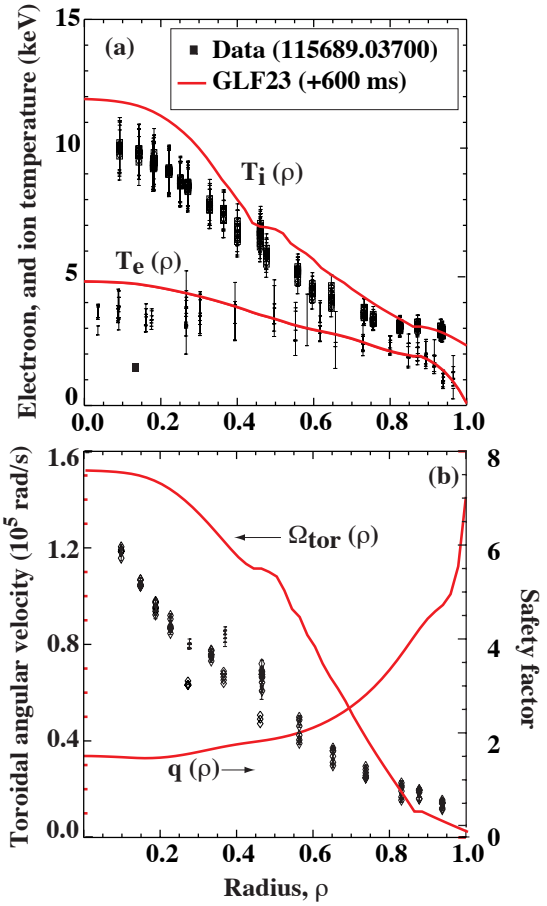

Fig. 5. GLF23 simulation of an AT discharge with a large NBI power demand: Shot 115689 I_p = 1.2 MA, B_T = 1.85 T, H_{89} = 1.9, β_N = 3.2, P_{NBI} = 14.4 MW. The model predictions substantially over-estimate the experimental profiles, particularly for the toroidal angular rotation velocity.

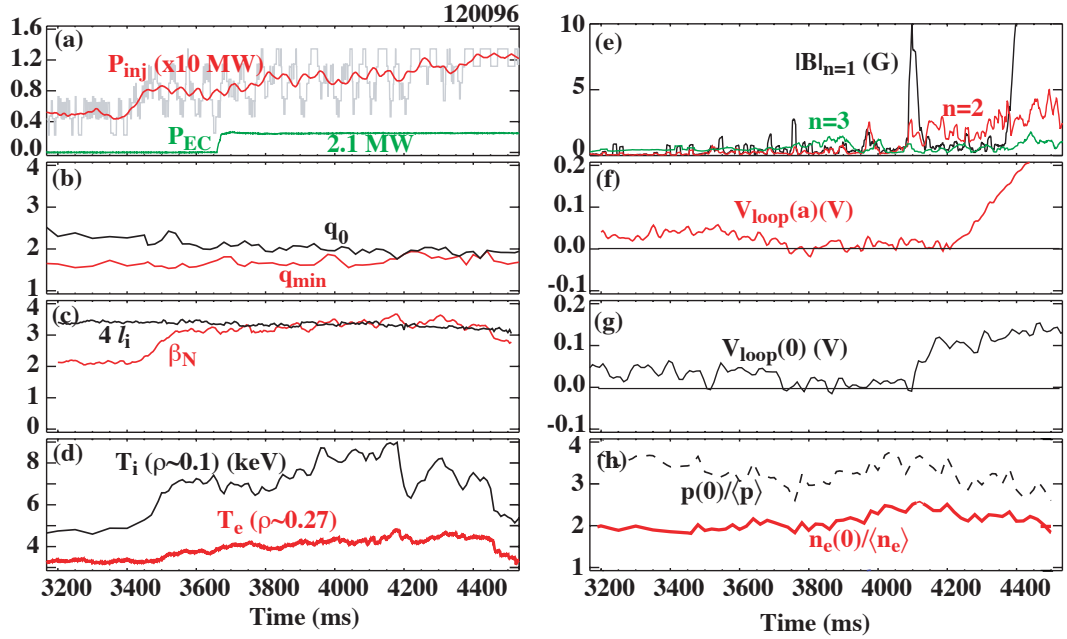

Fig. 6. Evolution of discharge characteristics of a recent AT discharge with $f_{NI} \approx 100\%$, $\beta_N \approx 3.5$. Both axial and edge loop voltage are close to zero. The favorable state was terminated by n=1 MHD activity at 4.35 s.

amplitude, sustained n=1 mode appeared (at 4350 ms), while the axial loop voltage was low until a fast growing n=1 mode appeared at 4125 ms.

The n=1 MHD is ideally unstable as a consequence of pressure profile peaking from the spontaneous formation of an internal transport barrier. The ideal MHD is thought to be responsible for triggering the NTMs. During the high β phase, the n=3 (m=5) mode first appeared as q_{min} dropped below 1.7. This was followed by the n=2 and n=1 modes, leading to a fast growing n=1 mode at t = 4125 ms. The evolution of the $q(\rho)$ profile is approximately consistent with the sequence of the observed frequencies of tearing modes and measured toroidal rotation profile. Stability analysis of the fast growing mode using GATO, DCON, and PEST-III all indicated an n=1 ideal instability [23]. The cause of the instability is pressure peaking, predominantly due to the density peaking, as shown by peaking factors in Fig. 6(h). The MHD activity is typical for β_N above the no-wall limit and q_{min} between 1.5 and 1.7. Detailed analysis of resistive stability was carried out using the PEST-III code based on a series of equilibria, and showed the sensitivity of Δ' to details of equilibrium reconstructions, as the ideal instability boundary is approached, as observed previously [10,24]. The onset of the n=1 ideal instability provided seeds for growth and saturation of the subsequent m/n=3/2 NTMs, ending up with the saturated n=1 mode, which caused the aforementioned confinement degradation.

f_{NI} = 100% was maintained throughout ITB formation until the ideal n=1 mode appeared as shown in Fig. 7. The confinement was excellent with low P_{NB} demand. Bootstrap current and NB and ECCD sources were well-aligned, as evidenced by the local Ohmic current being close to zero throughout the profile as shown in Fig. 8(a). The ideal n=1 interchange mode moved the off-axis current sources inward, as clearly seen in the time traces of individual MSE channels [25] and also comparison of the toroidal current profile $J_\phi(R)$ from MSE before and after the n=1 mode shown in Fig. 8(b). Nevertheless the alignment of NI sources remained excellent. With the n=1 mode continued (t > 4350 ms), NBCD from higher P_{NB} compensated the reduction of bootstrap current due to confinement deterioration, resulting in the net J_{NI} remained 100%, although the good alignment was lost.

Stable operation at β_N = 3.4 for 2 s was obtained without significant MHD. In some cases, β_N up to 4 was obtained transiently. Efforts to further optimize these plasmas will benefit from the anticipated (1) higher power, longer duration gyrotron, (2) development of feedback control of the current profile, and (3) application of fast wave

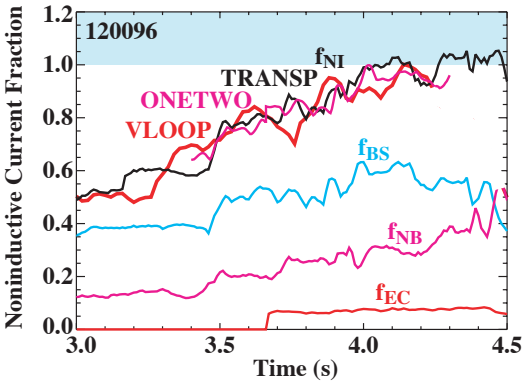

Fig. 7. The 100% noninductive fraction was obtained for ≈200 ms with good alignment of noninductive current sources before the fast growing n=1 MHD. The high NBI power demand during sustained MHD held a net 100% noninductive fraction, but the good alignment was lost.

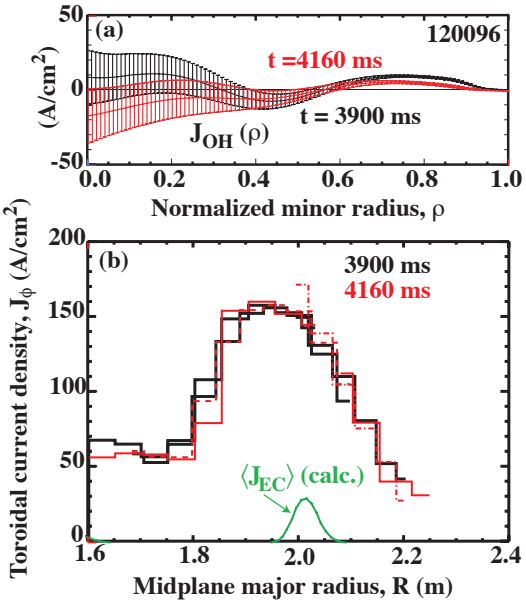

Fig. 8. Comparison of (a) Ohmic current density profiles before and after n=1 MHD, and (b) toroidal current densities measured by a motional Stark effect diagnostic at two different times, before and after the ideal n=1 mode. Except for small inward movement of the off-axis current, both profiles show well-aligned noninductive current sources making Ohmic current close to zero everywhere.

heating and current drive for improved heating for high ECCD efficiency and controlling the central shear, and possibly reducing density peaking.

3. Predictive Modeling for Steady-State Performance

The scientific basis being developed on DIII-D is leading to increased confidence in establishing steady-state operational scenarios for ITER and beyond. High bootstrap fraction, steady-state, high performance operation involves complex nonlinear interaction amongst the key physics elements and requires detailed code models to predict performance in larger tokamaks. A computational advance recently incorporated in the ONETWO transport code is the use of a globally convergent nonlinear solution method based on a combination of the steepest descent and modified Newton method. The method is applied both to time-dependent and time-independent versions of the transport equations, but the time-independent version is of particular value for modeling the steady-state behavior of current drive plasmas due to the long parallel electric field equilibration time. Simulation of the f_{NI} = 90% case in DIII-D (Fig. 4) shows a small drop in the central safety factor q_0 due to the fully penetrated Ohmic current with little change in other profiles.

This unique capability was applied to simulation of the ITER steady-state reference scenario with the Day-1 heating and current drive capabilities. The objective of this simulation is to seek an existence proof of a steady state solution for 100% noninductive operation using the GLF23 theory-based model with self-consistent source and sink calculations. Since the core performance depends strongly on the edge temperature due to the stiff transport model, scans of an assumed edge temperature value are used to determine the required edge temperature for achieving the goal of the steady state scenario (100% noninductive current fraction with f_{BS} >0.5). The results indicated that the projected performance can be met with T (ρ=0.9) of 7 keV with some uncertainties of bootstrap models shown in Fig. 9. The radial profiles of the simulation for the 100% noninductive fraction case are reported in [27]. The parallel electric field is fully penetrated and the Ohmic current is (within the perceived accuracy of the modeling) essentially zero with a loop voltage of ~1 mV. These parameters correspond to the 0-D operation space of the ignition figure of merit, $\beta_N H_{89}/q_{95}^2 = 0.33$ with $f_{BS} \approx 80\%$. More iterations and optimization need to be carried out to make the current profile evolution fully consistent.

4. Summary and Future Work

100% noninductively driven plasmas have been achieved with β_T up to 3.6%, β_N up to 3.5, and $H_{89} \sim 2.3$. The limitation of the high performance discharges is the current profile evolution to unstable states, in particular, leading to RWMs and NTMs. An advanced plasma control system is crucial to control the current profile evolution. These experiments have achieved an ignition figure of merit $H_{89}\beta_N/q_{95}^2 \approx 0.3$ with bootstrap current fraction $f_{BS} \approx 60\%$, consistent with requirements for the ITER Q=5 steady-state scenarios. The modeling tools that were successfully employed to devise experiments in DIII-D are applied to ITER, indicating full noninductive operation is plausible for an ITER steady state scenario with $Q > 7$.

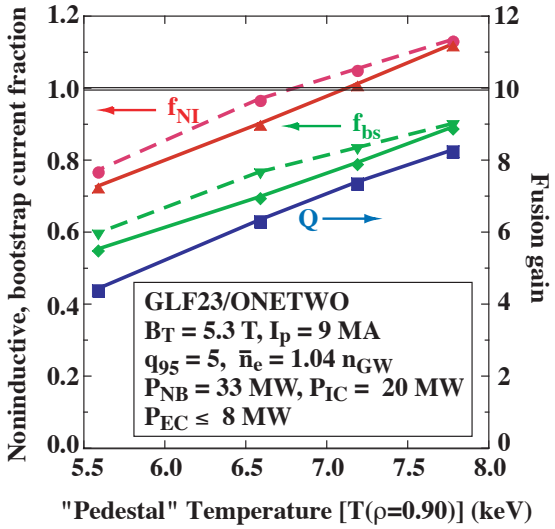

Fig. 9. Application of the GLF23 predictive simulation for steady-state performance of the ITER AT scenario. Variation of the noninductive current fraction, f_{NI}, and bootstrap current fraction, f_{BS}, and fusion gain, Q, is shown with edge temperature at ρ=0.9. The bootstrap current is based on Sauter (dashed) and NCLASS (solid) models.

Several hardware improvements are planned to foster further advances in the science of Advanced Tokamaks. A double-null pumped divertor will allow operation with density control in an optimized shape [22]. Additional rf power is planned, with increases to six 1 MW class gyrotrons of EC and 4 MW of fast wave. This will allow demonstration of steady state regimes for as long as 10 seconds, or several current relaxation times. Replacing some of the NBI with rf will facilitate operation with $T_e/T_i \approx 1$, a more relevant regime for next-step burning plasmas. Finally, two (out of eight) NBI sources are planned to be re-aimed in the counter direction. This will give added flexibility by allowing us to vary the co/counter mix of NBI sources, thereby modifying both NBCD and rotation.

Acknowledgments

This work was supported by the U.S. Department of Energy under DE-AC05-00OR22725, DE-FC02-04ER54698, W-7405-ENG-48, DE-FG03-97ER54415, DE-AC05-76OR00033, DE-FG03-01ER54615, DE-AC02-76CH03073, and DE-FG02-89ER53297. We would like to thank the DIII-D Team. We also wish to acknowledge useful discussions with Drs. C. Gormezano and W.A. Houlberg. The modeling was carried out using Grid-enabled TRANSP on the National Fusion Grid, and we would like to thank the members at PPPL and GA of the National Fusion Collaboratory Project (www.fusiongrid.org) sponsored by the US DOE SciDAC Program.

References

[1] LUCE, T.C., *et al.,* this conference.
[2] BICKERTON, R.J., CONNOR, J.W., and TAYLOR, J.B., Nature (London), Phys. Sci., **229** (1971) 110.
[3] YUSHMANOV, P.N., TAKIZUKA, T., RIEDEL, K.S., *et al.,* Nucl. Fusion **30** (1990) 1999.
[4] LUCE, T.C., to be published in Fusion Tech Sci. (2004).
[5] OKABAYASHI, M., *et al.,* this conference.
[6] PETTY, C.C., *et al.,* this conference.
[7] SIPS, A.C.C., *et al.,* this conference.
[8] ITER Physics Basis, Nucl. Fusion **39** (1999) 2203.
[9] MIKKELSEN, D.R., Phys. Fluid B **1** (1989) 333.
[10] WADE, M.R., *et al.,* Nucl. Fusion **43** (2003) 634.
[11] MURAKAMI, M., *et al.,* Phy. Plasmas **10** (2003) 1691.
[12] MURAKAMI, M., ST JOHN, H.E., CASPER, T.A., *et al.,* Nucl. Fusion **40** (2000) 1257.
[13] WALTZ, R.E., STAEBLER, G.M., DORLAND, W., *et al.,* Phys. Plasmas **4** (1997) 2482.
[14] ST JOHN, H.E., TAYLOR, T.S., LIN-LIU, Y.R., and TURNBULL, A.D., Plasma Phys. and Control. Nucl. Fusion Research 1994, in Proc. of the 15th IAEA Conference, Seville, 1994, Vol. 3 (IAEA, Vienna, 1994) p. 603.
[15] HAWRYLUK, R.J., "An empirical approach to tokamak transport," in *Physics Close to Thermonuclear Conditions*, edited by B. Coppi *et al.* (Commission of the European Communities, Brussels, 1980), Vol. 1, p. 19.
[16] HOULBERG, W.A., SHAING, K.C., HIRSHMAN, S.P., ZARNSTORFF, M.C., Phys. Plasmas **4** (1997) 3230.
[17] SAUTER, O., ANGIONI, C., and LIN-LIU, Y.R., Phys. Plasmas **6** (1999) 2834.
[18] MATSUDA, K., IEEE Trans. Plasma Sci. **17** (1989) 6.
[19] LAO, L.L., FERRON, J.R., GROEBNER, R.J., *et al.,* Nucl. Fusion **30** (1990) 1035.
[20] FOREST, C.B., KUPFER, K., LUCE, T.C., *et al.,* Phys. Rev. Lett. **73** (1994) 2444.
[21] KINSEY, J.E., STAEBLER, G.M., WALTZ, R.E., Fusion Sci. Technol. **44** (2003) 763.
[22] GREENFIELD, C.M., MURAKAMI, M., FERRON, J.R., *et al.,* to be published in Plasma Phys. Control. Fusion (2004).
[23] FERRON, J.R., *et al.,* this conference.
[24] BRENNAN, D.P., STRAIT, E.J., TURNBULL, A.D., *et al.,* Phys. Plasmas **9** (2003) ?
[25] RICE, B.W., BURRELL, K.H., LAO, L.L., LIN-LIU, Y.R., *et al.,* Phys. Rev. Lett. **79** (1997) 2694.
[26] SHIMADA, M., *et al.,* this conference.
[27] HOULBERG, W.A., *et al.,* this conference.